

On the discovery potential of the lightest MSSM Higgs Boson at the LHC

R. Kinnunen[†], S. Lehti[†], A. Nikitenko^{‡§} and P. Salmi^{†||}

[†] Helsinki Institute of Physics, Helsinki, Finland

[‡] Imperial College, University of London, London, UK

Abstract. Production of the lightest MSSM Higgs boson h is studied at the LHC. Isorate contours for the $h \rightarrow \gamma\gamma$ and $h \rightarrow \tau^+\tau^-$ decay channels are shown in the $(m_A, \tan\beta)$ parameter space. Effects of the SUSY parameters, in particular the stop mixing and stop quark mass, are investigated. Search strategies at the LHC are discussed and the discovery potential is calculated for the CMS experiment. The MSSM parameter space for $m_A \gtrsim 150\text{-}200 \text{ GeV}/c^2$ is expected to be covered with at least one decay channel with an integrated luminosity of 60 fb^{-1} . A light stop quark with large stop mixing can affect seriously the discovery potential in the $h \rightarrow \gamma\gamma$ and $h \rightarrow ZZ^*$ decay channels.

1. Introduction

The Minimal Supersymmetric Standard Model (MSSM) contains five Higgs bosons: a light CP-even Higgs boson h , a heavy CP-even Higgs boson H , a CP-odd Higgs boson A and two charged Higgs bosons H^\pm . At tree-level the h (H) mass is bound to be below (above) the Z boson mass. The higher order corrections increase this upper (lower) bound, the largest possible value being about $135 \text{ GeV}/c^2$ [1]. The fact that in the MSSM one Higgs boson is bound to be light gives a strong prediction for the mass region where the lightest Higgs boson might be seen.

The LEP and Tevatron results have already constrained the MSSM parameter space significantly. The measurements yield lower bounds of 91.0 and $91.9 \text{ GeV}/c^2$ for the lightest CP-even Higgs boson h and for the CP-odd A , respectively [2]. The excluded $\tan\beta$ regions are $0.5 < \tan\beta < 2.4$ for the maximal m_h scenario (maximal mixing scenario) and $0.7 < \tan\beta < 10.5$ for the no-stop-mixing scenario [2], assuming top quark mass $174.3 \text{ GeV}/c^2$. The recent results from the Tevatron, however, give the world average for the top mass of $178.0 \pm 4.3 \text{ GeV}/c^2$ [3]. The larger top mass softens the bounds, for example assuming the top mass of $179.3 \text{ GeV}/c^2$ the excluded region by LEP in the maximal mixing scenario is $0.9 < \tan\beta < 1.5$ and for top mass of about $183 \text{ GeV}/c^2$ the exclusion vanishes [4]. Some constraints have been derived from

[§] On leave from ITEP, Moscow, Russia

^{||} Present address: Instituut-Lorentz, Leiden University, The Netherlands

the existing data for the other SUSY parameters. The value of the trilinear coupling A_t is limited to $350 \text{ GeV}/c^2 \lesssim A_t \lesssim 1.5 (2.3) \text{ TeV}/c^2$ for a light stop quark with $m_{\tilde{t}_1} = 200 (400) \text{ GeV}/c^2$ and for the experimental constraint $m_h \gtrsim 90 \text{ GeV}/c^2$ [5]. The higgsino and gaugino mass parameters μ and M_2 are related to neutralino and chargino masses, and experimental mass bounds can be used to exclude $|\mu|$ and M_2 values below $100 \text{ GeV}/c^2$ [6]. The present experimental lower bound from LEP for the stop quark mass is $\sim 100 \text{ GeV}/c^2$ [7]. The mass limit from the Tevatron RunII with the ultimate luminosities ($\sim 20 \text{ fb}^{-1}$) is expected to reach $m_{\tilde{t}_1} \sim 240 \text{ GeV}/c^2$ [8].

In this work three SUSY scenarios are considered: a no-mixing scenario where the mixing of the left and right handed stop eigenstates do not play any significant role and where all SUSY particles are assumed to be heavy [9], a maximal-mixing scenario which maximizes the h mass [9], and a light-stop scenario in which the stop quark mass is of the same order as the top quark mass [5]. These scenarios do not assume any particular model for the soft SUSY-breaking mechanism. The stop mixing parameter is defined as $X_t = A_t - \mu \cot \beta$, with A_t being the trilinear Higgs-stop coupling. The stop-mixing is maximized when $X_t = \sqrt{6} \times M_{\text{SUSY}}$, where M_{SUSY} is the heavy SUSY scale [9]. In this work, the maximal stop-mixing scenario is defined taking $A_t = \sqrt{6} \times M_{\text{SUSY}}$, with $M_{\text{SUSY}} = 1 \text{ TeV}/c^2$. With respect to the standard definition, this choice leads to a deviation of less than 1% in the total production rate of $pp \rightarrow h + X$, $h \rightarrow \gamma\gamma$ at the LHC. No sbottom mixing is assumed taking $A_b = 0$. The higgsino mass parameter μ is set to $300 \text{ GeV}/c^2$ and the gaugino mass parameter M_2 is set to $200 \text{ GeV}/c^2$, values chosen large enough not to be already experimentally excluded. All the soft SUSY breaking mass parameters are set to $1 \text{ TeV}/c^2$, and the gluino mass $M_{\tilde{g}}$ is set to $800 \text{ GeV}/c^2$. The mass of the top quark is set to $175 \text{ GeV}/c^2$. The values of these parameters are taken to be the same in the no-mixing scenario, except that of the trilinear coupling A_t which is set to zero. For the light-stop scenario A_t is taken to be $1400 \text{ GeV}/c^2$ close to the highest possible experimentally allowed value ($A_t = 1500 \text{ GeV}/c^2$) with light stop quarks [5]. In this scenario μ is set to $-250 \text{ GeV}/c^2$ and M_2 to $250 \text{ GeV}/c^2$. The soft SUSY breaking mass parameters are set to $1 \text{ TeV}/c^2$ except the mass parameters of the stop sector, which are required to be of the order of $500 \text{ GeV}/c^2$ to allow the stop quark to be light. The actual value of the stop sector soft SUSY breaking mass parameters vary depending on the chosen stop quark mass.

With the above values of the SUSY parameters the upper bound of m_h is about $127 \text{ GeV}/c^2$ in the maximal-mixing scenario and about $114 \text{ GeV}/c^2$ in the no-mixing scenario. The sign of μ has only a small effect on the mass of the lightest Higgs boson. In the light-stop scenario with $m_{\tilde{t}_1} = 200 \text{ GeV}/c^2$, the upper bound of m_h is $113 \text{ GeV}/c^2$, as in the no-mixing scenario. For $m_{\tilde{t}_1} = 300 \text{ GeV}/c^2$ this upper bound increases by $10 \text{ GeV}/c^2$ approaching to that of the maximal-mixing scenario.

The $H \rightarrow \gamma\gamma$ channel is considered one of the major discovery channels for a light Standard Model (SM) Higgs boson and for the lightest scalar MSSM Higgs boson at the LHC. There can be, however, regions of the MSSM parameter space where this discovery potential is reduced. The effect of a light stop quark in the presence of large mixing

has been calculated and the consequences for the $gg \rightarrow h \rightarrow \gamma\gamma$ channel have been discussed in Ref. [5]. An experimental study was performed in Ref. [10] and the discovery potential was calculated for the $h \rightarrow \gamma\gamma$ channel in the CMS detector. In this earlier work, however, only the gluon-gluon fusion production process was simulated and other Higgs boson decay channels were not considered. In the present work, all significant production processes are included in the calculation of the inclusive $h \rightarrow \gamma\gamma$ rate in the MSSM and the discovery potential is evaluated also in the associated production and weak gauge boson fusion production processes $qq \rightarrow qqh$. Furthermore, updated programs are used to calculate the cross sections and branching ratios.

The aim of this paper is to extend the study of the loop effects in the $h \rightarrow \gamma\gamma$ channel to the full discovery potential of the lightest scalar Higgs boson at the LHC. Therefore, the $h \rightarrow ZZ^* \rightarrow \ell^+\ell^-\ell'^+\ell'^-$ and $h/H \rightarrow \tau^+\tau^-$ decay channels were also studied. The $h \rightarrow ZZ^* \rightarrow \ell^+\ell^-\ell'^+\ell'^-$ has not been so far considered as a discovery channel in the MSSM at large $\tan\beta$. It is shown, however, in Section 3.2 that this channel can yield a large discovery potential if the SUSY scenario is such that $m_h^{\max} \gtrsim 125 \text{ GeV}/c^2$. The $h/H \rightarrow \tau^+\tau^-$ decay channels with lepton+jet and two-lepton final states in the weak gauge boson fusion production have been shown to be particularly interesting and to cover the full of the MSSM parameter space [11]. In this paper the discovery potential for this channel is calculated with realistic detector sensitivities. The CMS detector sensitivities are used and were obtained from the recent simulations for the discovery potential of a light SM Higgs boson [12].

2. Phenomenology

2.1. Production cross sections

The lightest MSSM Higgs boson h is produced through the gluon fusion $gg \rightarrow h$, the associated processes $q\bar{q}/gg \rightarrow t\bar{t}h$, $q\bar{q}/gg \rightarrow b\bar{b}h$, $qq \rightarrow Wh/Zh$ and through the weak gauge boson fusion process $qq \rightarrow qqh$. The gluon fusion process dominates the production over the entire parameter space. This process is mediated by heavy quark and squark triangle loops. The cross sections to the leading order (LO) and to the next to leading order (NLO) are calculated in this work with the program HIGLU [13]. The top and bottom loops are included in the calculation of the Higgs boson coupling to gluons in this program. Since the squark loops are not included, the decay width $\Gamma(h \rightarrow gg)$, calculated with the HDECAY program [14], is used to include the squark loop effects: the cross section given by HIGLU is divided by the decay width $\Gamma(h \rightarrow gg)$ with sparticle loops switched off, and multiplied by the decay width with all sparticle effects. The Higgs boson mass is kept constant in this procedure. The corrected gluon fusion cross section with SUSY loop effects can be presented with the respective branching ratios and total widths as

$$\sigma \cdot \text{BR} = \sigma(gg \rightarrow h) \cdot \frac{\text{BR}(h \rightarrow gg)^{\text{susy}}}{\text{BR}(h \rightarrow gg)^{\text{nosusy}}} \frac{\Gamma_{\text{TOT}}^{\text{susy}}}{\Gamma_{\text{TOT}}^{\text{nosusy}}} \cdot \text{BR}(h \rightarrow \gamma\gamma)_{\text{susy}}, \quad (1)$$

Table 1. Production cross sections for the lightest MSSM Higgs boson for $m_h = 125.8 \text{ GeV}/c^2$ ($m_A = 250 \text{ GeV}/c^2$) and $\tan\beta = 10$ with maximal stop mixing.

process	$gg \rightarrow h$	$qq \rightarrow qqh$	$qq \rightarrow Wh$	$qq \rightarrow Zh$	$pp \rightarrow b\bar{b}h$	$pp \rightarrow t\bar{t}h$	σ_{TOT}
σ (pb)	27.3	4.17	1.59	0.64	0.72	0.32	34.1
$\sigma/\sigma_{\text{TOT}}$	79%	12%	4.6%	1.8%	2.1%	0.9 %	100 %

where `nosusy` refers to the branching ratio and total width calculated assuming heavy SUSY particles and `susy` to the same variables with SUSY spectrum determined by the given scenario.

The cross sections for the associated production with weak gauge bosons $qq \rightarrow Wh$ and $qq \rightarrow Zh$ are calculated with the program V2HV [15] to both leading and next to leading order. The cross sections for the production with associated quark pairs $q\bar{q}/gg \rightarrow t\bar{t}h$ and $q\bar{q}/gg \rightarrow b\bar{b}h$ are calculated with the HQQ program [15], which presently includes only the LO processes. The cross sections for the weak gauge boson fusion $qq \rightarrow qqh$ are evaluated with the VV2H program [15]. The production cross sections and the contributions from the individual production processes to the total cross section at $m_h = 125.8 \text{ GeV}/c^2$ ($m_A = 250 \text{ GeV}/c^2$), $\tan\beta = 10$ are shown in Table 1. The gluon fusion process contributes about 80% to the total cross section. This fraction is not sensitive to the Higgs boson mass and $\tan\beta$.

In the SM, the K-factor (defined as $K = \sigma_{\text{NLO}}/\sigma_{\text{LO}}$) for the gluon fusion process is large varying between 1.5 and 1.7 [16]. In the MSSM, this K-factor depends on $\tan\beta$ being about the same as in the SM at small $\tan\beta$ and closer to unity at large $\tan\beta$ [16]. The K-factors do not depend significantly on the squark mass and are stable against the loop effects in the gluon fusion mechanism even in the extreme situation when one of the stop mass eigenstates is light while the other squarks are heavy and decouple [17]. The K-factor in the associated process $qq \rightarrow Wh$ is almost independent of m_A and $\tan\beta$ and is about 1.3 for both the no-mixing and maximal-mixing scenario.

2.2. Decay channels

Figures 1 and 2 show the branching ratios for the lightest MSSM Higgs boson as a function of m_A and m_h with maximal stop quark mixing for $\tan\beta = 10$ and 30, respectively. The branching ratios and decay widths are calculated with the program HDECAY 3.0 [14]. The next to leading order (NLO) values are used for the decay modes throughout this study. The $h \rightarrow b\bar{b}$ decay channel dominates. The branching ratios to weak gauge bosons $h \rightarrow ZZ^*$ and $h \rightarrow WW^*$ increase rapidly when m_h approaches its maximum value reaching $\sim 2\%$ and $\sim 20\%$, respectively, at large m_A . For $m_A \gtrsim 200 \text{ GeV}/c^2$ the branching ratio for the $h \rightarrow \gamma\gamma$ decay channel is between one and two per mil. The branching ratios for the $h \rightarrow \tau^+\tau^-$, $h \rightarrow b\bar{b}$ and $h \rightarrow \mu^+\mu^-$ decay channels remain large also for $m_A \lesssim 200 \text{ GeV}/c^2$, where the lightest Higgs boson is not SM-like, due to the enhanced couplings to the down type fermions.

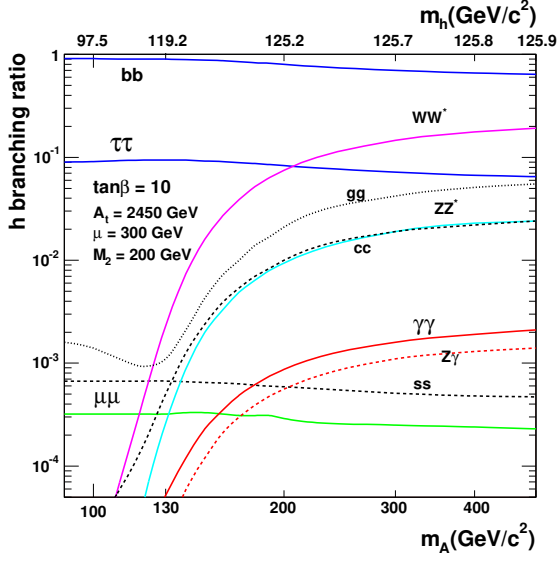


Figure 1. Branching ratios for the lightest MSSM Higgs boson as a function of m_A and m_h for $\tan\beta = 10$ with maximal stop quark mixing.

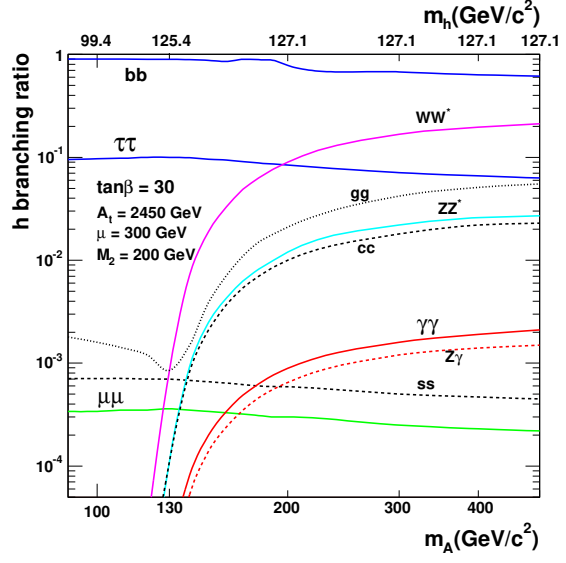


Figure 2. The same as in Fig. 1 but for $\tan\beta = 30$.

2.3. Effect of SUSY parameters

In the MSSM, one of the stop quarks may become much lighter than the other squarks if mixing between different squark isospin eigenstates is large. The mixing can be described with the following mass matrix [18]

$$\begin{pmatrix} m_{\tilde{t}_L}^2 & m_{\text{top}}(A_t - \mu \cot\beta) \\ m_{\text{top}}(A_t - \mu \cot\beta) & m_{\tilde{t}_R}^2 \end{pmatrix} \quad (2)$$

where \tilde{t}_L and \tilde{t}_R are the left and right handed eigenstates of the stop quark and $A_t - \mu \cot\beta \equiv X_t$ is the squark mixing parameter with A_t being the trilinear coupling and μ the higgsino mass parameter. Mixing in the third generation squark sector may be important, since, as seen from the off-diagonal terms of the mass matrix, the squark mixing is proportional to the corresponding quark mass. For a heavy top quark, mixing in the stop sector may thus produce considerable splitting between the mass eigenstates \tilde{t}_1, \tilde{t}_2

$$m_{\tilde{t}_{1,2}}^2 = \frac{1}{2}(m_{\tilde{t}_L}^2 + m_{\tilde{t}_R}^2) \mp \frac{1}{2}\sqrt{(m_{\tilde{t}_L}^2 - m_{\tilde{t}_R}^2)^2 + 4m_{\text{top}}^2(A_t - \mu \cot\beta)^2} \quad (3)$$

resulting in one very light and one very heavy stop quark. In above relations $m_{\tilde{t}_L}^2 = M_{\tilde{Q}}^2 + m_Z^2 \cos 2\beta (I_3^{\tilde{t}} - e_{\tilde{t}} \sin^2 \theta_W) + m_{\text{top}}^2$ and $m_{\tilde{t}_R}^2 = M_{\tilde{U}}^2 + m_Z^2 \cos 2\beta e_{\tilde{t}} \sin^2 \theta_W + m_{\text{top}}^2$ where $M_{\tilde{Q}}$ and $M_{\tilde{U}}$ are the soft-SUSY breaking scalar masses, $I_3^{\tilde{t}}$ is the squark weak isospin and $e_{\tilde{t}}$ the squark charge. It can be seen that in order to have large splitting between the two stop eigenstates and therefore a light stop quark, X_t must be large. For a common scalar mass parameter of 1 TeV, the mass of the lighter stop quark is of the order of

800 GeV/c². A light stop quark ($m_{\text{stop}} \lesssim 300$ GeV/c²) can be obtained choosing the third generation scalar masses $M_{\tilde{U}}$ and $M_{\tilde{Q}}$ to be of the order of 500 GeV/c². For these parameter values, the mass of the lightest supersymmetric particle LSP is of the order of 100 GeV/c², well above the present experimental limit [2]. In the next sections, the lighter of the two stop mass eigenstates is denoted simply as a stop quark, $\text{stop} \equiv \tilde{t}_1$ and its mass m_{stop} .

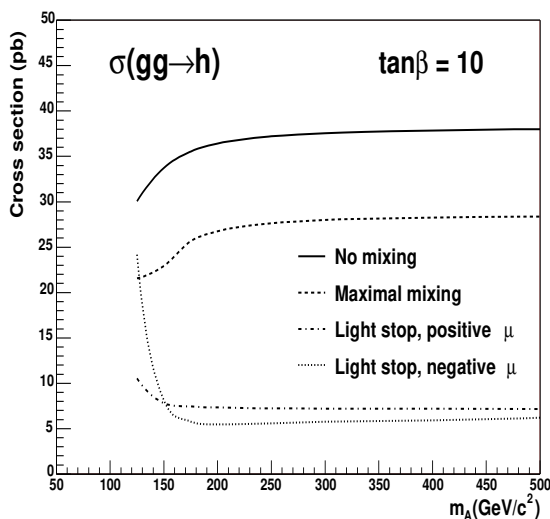


Figure 3. Cross section for the $gg \rightarrow h$ process with $\tan\beta = 10$ without stop mixing, with maximal stop mixing and with light stop quark $m_{\text{stop}} = 200$ GeV/c² for $\mu < 0$ and for $\mu > 0$.

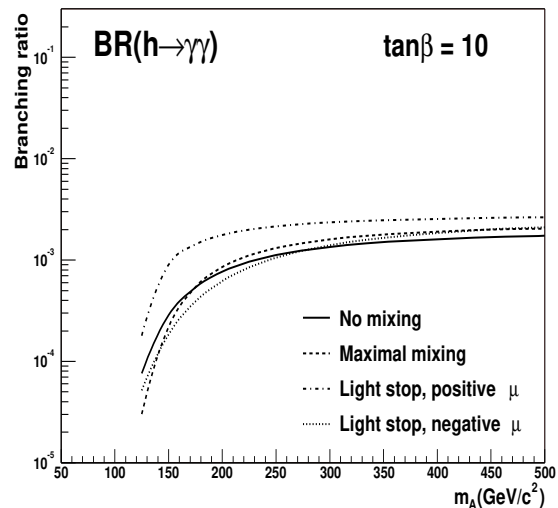


Figure 4. The branching ratio for the $h \rightarrow \gamma\gamma$ decay with $\tan\beta = 10$ without stop mixing, with maximal stop mixing and with light stop quark $m_{\text{stop}} = 200$ GeV/c² for $\mu < 0$ and for $\mu > 0$.

Since no supersymmetric particles have been found so far, the supersymmetry must be broken, the squarks do not have the same masses as quarks and the cancellation at loop level is less significant. The results from existing experiments indicate that a scenario with large mixing in the squark (stop) sector is possible and more likely than a no-mixing scenario [2]. If the mass of the stop quark is small, of the order of the top quark mass, the cancellation effects become important.

It has been first shown in Refs. [5, 19] that the rate for the $gg \rightarrow h \rightarrow \gamma\gamma$ process could be strongly reduced with large mixing and with a light stop quark ($m_{\text{stop}} \sim m_{\text{top}}$). The top - stop interference leads to a suppression of the top quark contribution in the loops mediating the Higgs boson production, since the stop loop interferes destructively with the top quark and the top and stop loops partly cancel. The loop mediated Higgs boson decay into photons is also affected, but since the dominant contribution comes now from a W loop, which interferes destructively with the top loop, a reduction of the top contribution by interfering stop loops increases the $h \rightarrow \gamma\gamma$ partial width. As the

W loop dominates in this partial width, the interference effect is smaller than in the $gg \rightarrow h$ process dominated by a top quark loop. In addition to the light stop, there are contributions from the charged Higgs bosons, sfermions and especially from charginos, but their net effect to the $h \rightarrow \gamma\gamma$ partial width is small, less than $\sim 10\%$ [20]. At large $\tan\beta$ also the bottom loop contributes and even becomes larger than the top loop contribution [21]. As the reduction of the $gg \rightarrow h$ partial width is significantly stronger than the enhancement of the $h \rightarrow \gamma\gamma$ partial width, the rate for $gg \rightarrow h \rightarrow \gamma\gamma$ is reduced. For $m_A \gtrsim 100 \text{ GeV}/c^2$, $A_t = 1.5 \text{ TeV}/c^2$, $m_{\text{stop}} = 200 \text{ GeV}/c^2$ and $\mu = 300 \text{ GeV}/c^2$ the rate is reduced by a factor of ~ 10 relative to the no-mixing scenario with heavy SUSY particles. The squark sector can affect the branching ratios of the lightest Higgs boson only via this interference phenomenon because the decays into gauginos are not kinematically allowed.

Figure 3 shows the cross section for the $gg \rightarrow h$ process and Fig. 4 the branching ratios for the $h \rightarrow \gamma\gamma$ decay channel corrected for the loop effects for the following scenarios: no stop mixing, maximal stop mixing, light stop quark $m_{\text{stop}} = 200 \text{ GeV}/c^2$ with $\mu < 0$ and light stop quark $m_{\text{stop}} = 200 \text{ GeV}/c^2$ with $\mu > 0$. The interference between the stop and top quarks is clearly visible: the lighter the stop quark the stronger the interference and smaller the cross section.

At large $\tan\beta$ the b couplings are enhanced, but the contributions from the sbottom loops are suppressed compared to the bottom loops by $(m_b/m_{\tilde{b}_j})^2$ [17]. With the LEP lower bound for the sbottom mass [22], the contribution is on a per mille level. In this work the mixing in the sbottom sector is not considered.

2.4. Search strategies

In the expected mass range, $m_h \lesssim 135 \text{ GeV}/c^2$, the lightest MSSM Higgs boson h can be searched for through the following decay channels: $h \rightarrow \gamma\gamma$, $h \rightarrow \gamma Z$, $h \rightarrow \mu^+\mu^-$, $h \rightarrow b\bar{b}$, $h \rightarrow ZZ^* \rightarrow \ell^+\ell^-\ell'^+\ell'^-$, $h \rightarrow WW^* \rightarrow \ell^+\ell^-\nu_\ell\nu_\ell$ and $h \rightarrow \tau^+\tau^-$. The searches in the $h \rightarrow \gamma\gamma$, $h \rightarrow \mu^+\mu^-$ and $h \rightarrow ZZ^* \rightarrow \ell^+\ell^-\ell'^+\ell'^-$ channels are based on the small total width of the Higgs boson in this mass range (in the SM and MSSM) exploiting the precise photon energy and lepton momentum measurements for the Higgs boson mass reconstruction [23, 24, 25]. The $h \rightarrow \gamma\gamma$ and $h \rightarrow ZZ^* \rightarrow \ell^+\ell^-\ell'^+\ell'^-$ channels are expected to yield their largest reaches in the inclusive production, dominated by the gluon fusion process. The $h \rightarrow \gamma\gamma$ channel can be searched for also in the associated production processes $t\bar{t}h$ and Wh with a requirement of an isolated lepton from the $W \rightarrow \ell\nu_\ell$ decay [26]. The signal-to-background ratios are larger but the event rates are smaller than for the inclusive production. For the $h \rightarrow b\bar{b}$ decay channel, suppression of the QCD multi-jet background is possible only in the associated production processes $t\bar{t}h$ and Wh with a requirement of an isolated lepton from the $W \rightarrow \ell\nu_\ell$ decay [27]. The $h \rightarrow \gamma\gamma$, $h \rightarrow \mu^+\mu^-$, $h \rightarrow WW^* \rightarrow \ell^+\ell^-\nu_\ell\nu_\ell$, $h \rightarrow \tau^+\tau^-$ and possibly $h \rightarrow b\bar{b}$ decay channels can be searched for also in the weak gauge boson fusion production process $qq \rightarrow qqh$. In this production mechanism tagging of the forward jets and vetoing on

central hadronic jets can be used to efficiently suppress the QCD multi-jet, W +jets and $t\bar{t}$ backgrounds [28]. The $h \rightarrow \tau^+\tau^-$ channel is particularly interesting in the MSSM as the couplings to down type fermions are $\tan\beta$ enhanced relative to SM couplings. Due to the tiny branching ratios, the $h \rightarrow \gamma Z$ and $h \rightarrow \mu^+\mu^-$ decay channels may be exploited only with the integrated luminosities exceeding 100 fb^{-1} .

3. Inclusive production channels

3.1. $h \rightarrow \gamma\gamma$

The isorate (cross section times branching ratio) curves for the $h \rightarrow \gamma\gamma$ channel in the inclusive production in the no-mixing scenario are shown in Fig. 5 with LO cross sections and in Fig. 6 with NLO cross sections. The isorate curves for the inclusive production in the maximal-mixing scenario are shown in Fig. 7 with LO and in Fig. 8 with NLO cross sections. Due to the larger Higgs boson mass m_h in the maximal-mixing scenario for fixed m_A and $\tan\beta$ the cross section is smaller than that in the no-mixing scenario. This decrease is compensated by a larger $h \rightarrow \gamma\gamma$ branching ratio resulting in a $\sim 3\%$ lower production (cross section times branching ratio) rate relative to the no-mixing scenario. Although in this scenario the stop quark is rather heavy $m_{\text{stop}} \simeq 800 \text{ GeV}/c^2$, the effect of the virtual stop loops suppresses the cross section by approximately 10% relative to the no-mixing scenario. A negative higgsino mass parameter would yield a further small suppression.

Figure 9 shows the cross section times branching ratio required for a 5σ statistical significance in the inclusive $h \rightarrow \gamma\gamma$ channel as a function of the invariant two-photon mass for 30 and 100 fb^{-1} in the CMS detector [23]. The NLO cross sections are assumed for the signal and backgrounds. In the mass range of the lightest MSSM Higgs boson, $m_h \lesssim 127 \text{ GeV}/c^2$, production rates at least 55 and 33 fb are needed to obtain a 5σ statistical significance with an integrated luminosities of 30 and 100 fb^{-1} , respectively. In the no-mixing scenario with $m_h \lesssim 114 \text{ GeV}/c^2$ the minimal production rates required for these luminosities are 71 and 42 fb, respectively. Larger rates are needed at lower mass values due to the increasing backgrounds. With these detector sensitivities a 5σ -discovery potential is expected for $m_A \gtrsim 200$ and $300 \text{ GeV}/c^2$ with integrated luminosities of 100 and 30 fb^{-1} , respectively. The reach is approximately the same in the no-mixing and maximal-mixing scenario.

Figures 10, 11 and 12 show the isorate curves for the $h \rightarrow \gamma\gamma$ channel in the light-stop scenario. Figure 10 shows the isorate curves for the dominating gluon fusion process which is affected most by a light stop quark. Figure 11 shows the isorate curves in the inclusive production for a very light stop quark, $m_{\text{stop}} = 200 \text{ GeV}/c^2$. Since the gluon fusion process is the dominating production mechanism, the effect of a light stop on the inclusive production is large, too. A discovery in the inclusive $h \rightarrow \gamma\gamma$ channel with such a light stop quark could be possible only for $m_A \gg 500 \text{ GeV}/c^2$ for integrated luminosities exceeding 100 fb^{-1} . Figure 12 shows the isorate curves for the

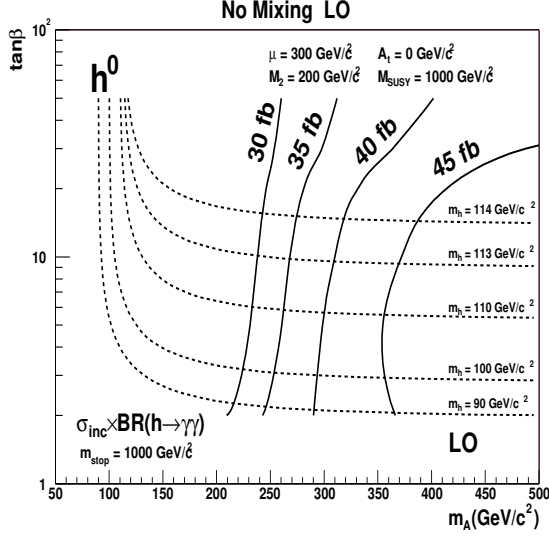


Figure 5. Isorate (cross section times branching ratio) curves for the inclusive $h \rightarrow \gamma\gamma$ channel in the no-mixing scenario with LO cross sections. The isomass curves for the lightest MSSM Higgs boson are shown with dashed lines.

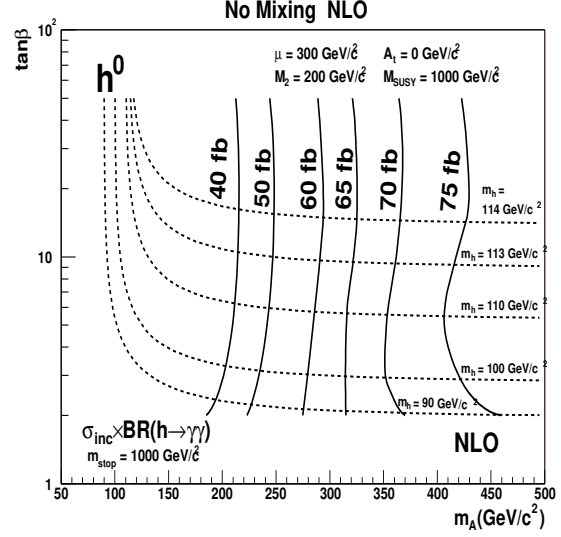


Figure 6. Isorate (cross section times branching ratio) curves for the inclusive $h \rightarrow \gamma\gamma$ channel in the no-mixing scenario with NLO cross sections. The isomass curves for the lightest MSSM Higgs boson are shown with dashed lines.

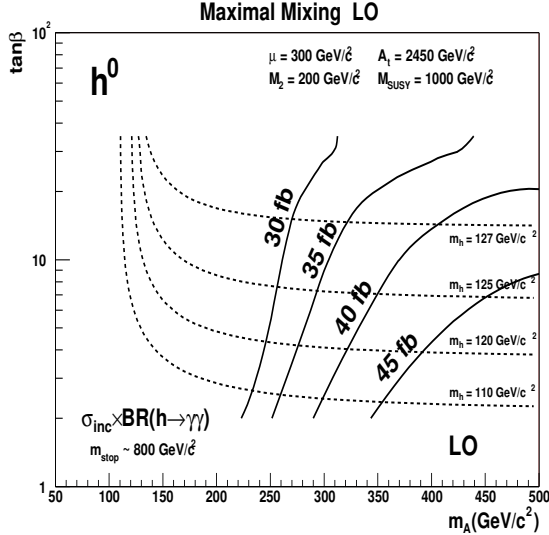


Figure 7. Isorate curves for the inclusive $h \rightarrow \gamma\gamma$ channel in the maximal-mixing scenario with LO cross sections.

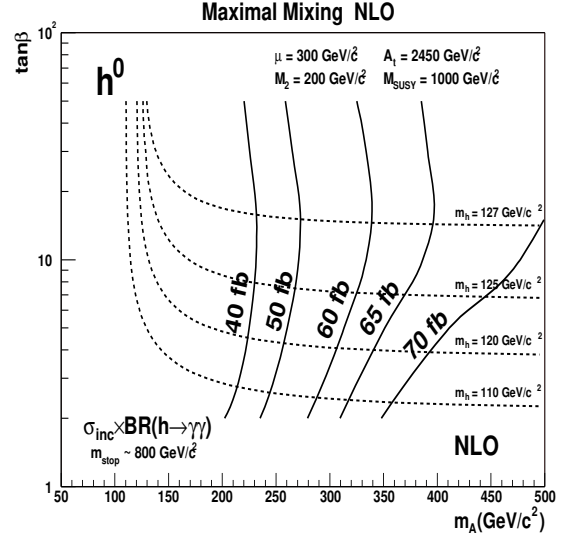


Figure 8. Isorate curves for the inclusive $h \rightarrow \gamma\gamma$ channel in the maximal-mixing scenario with NLO cross sections.

inclusive production with $m_{\text{stop}} = 300 \text{ GeV}/c^2$. For this value of m_{stop} a discovery is possible with 100 fb^{-1} in part of the parameter space for about $m_A \gtrsim 400 \text{ GeV}/c^2$ and

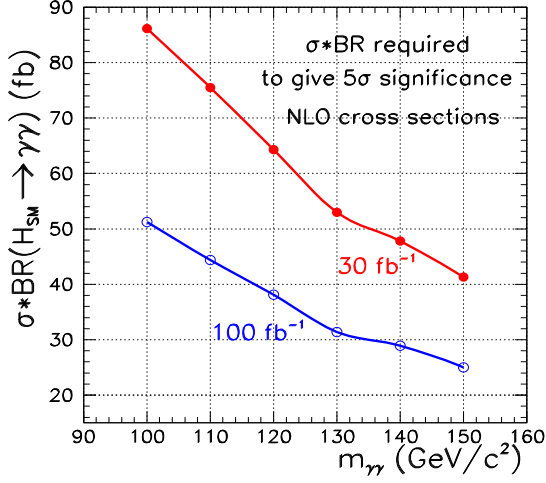


Figure 9. Cross section times branching ratio to give a 5σ statistical significance for the inclusive $H \rightarrow \gamma\gamma$ channel in the SM for 30 and 100 fb^{-1} assuming NLO cross sections for the backgrounds [23].

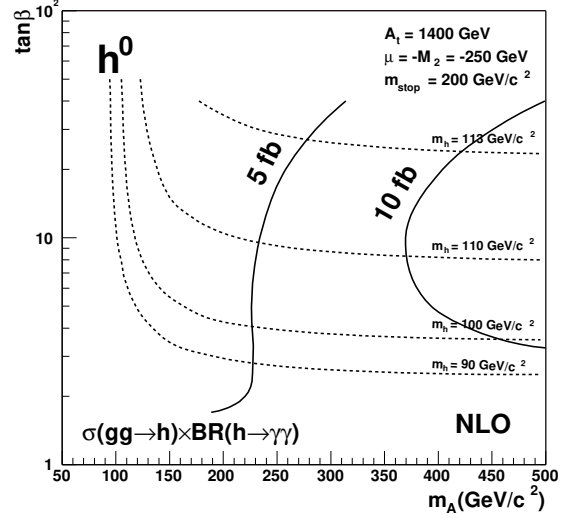


Figure 10. Isorate curves for the $gg \rightarrow h \rightarrow \gamma\gamma$ channel with a light stop quark $m_{\text{stop}} = 200 \text{ GeV}/c^2$ with LO cross sections.

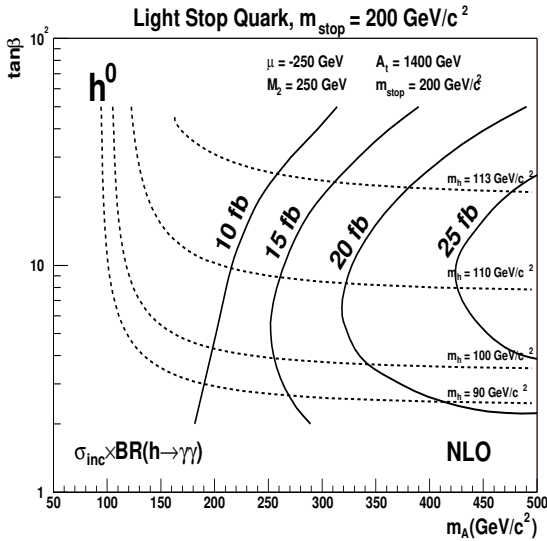


Figure 11. Isorate curves for the inclusive $h \rightarrow \gamma\gamma$ channel with a light stop quark $m_{\text{stop}} = 200 \text{ GeV}/c^2$ with NLO cross sections.

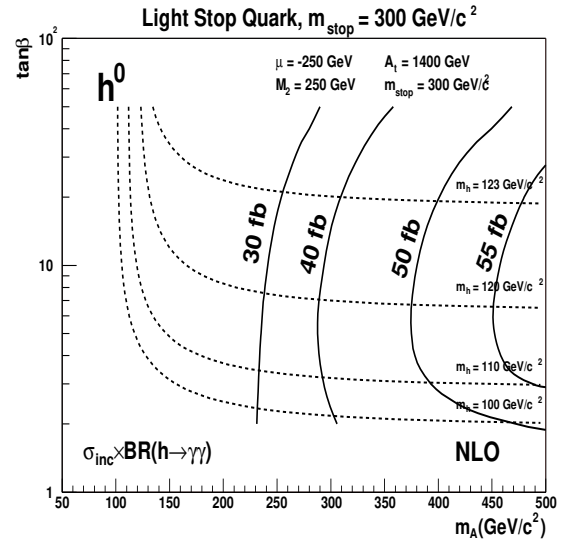


Figure 12. Isorate curves for the inclusive $h \rightarrow \gamma\gamma$ channel with a light stop quark $m_{\text{stop}} = 300 \text{ GeV}/c^2$ with NLO cross sections.

$\tan\beta \gtrsim 10$. For $m_{\text{stop}} \gtrsim 400 \text{ GeV}/c^2$ the interference effect is already small and the rate is close to that of the no-mixing and maximal-mixing scenarios.

3.2. $h \rightarrow ZZ^* \rightarrow \ell^+ \ell^- \ell'^+ \ell'^-$

The four-lepton channel, the $H \rightarrow ZZ^* \rightarrow \ell^+ \ell^- \ell'^+ \ell'^-$, has been shown to be the major discovery channel over the large mass rangion in the SM [12]. In the MSSM, the heavier scalar H could be searched for in the four-lepton channel at small $\tan\beta$. For $m_H \lesssim 2m_Z$, where the detector resolution dominates, the discovery potential could be obtained from that for the SM Higgs boson while for $m_H \gtrsim 2m_Z$ dedicated studies are needed due to the difference of total Higgs boson widths between the SM and MSSM in this region. For the lighter scalar h , a discovery could be possible close to the maximal possible value of m_h at large $\tan\beta$ and m_A . The discovery potential is strongly dependent on the lowest possible mass value accessible in the (pure) SM scenario, due to the fast decreasing $h \rightarrow ZZ^*$ branching ratio. The CMS studies have shown that this value could be as low as $m_H \sim 120 \text{ GeV}/c^2$ with an integrated luminosity of 100 fb^{-1} combining the electron and muon channels [29, 30]. Therefore a significant region at large $\tan\beta$ could be covered in the maximal-mixing scenario while no sensitivity is possible in the MSSM in the scenarios where the mass of the lighter scalar is below $\sim 120 \text{ GeV}/c^2$.

4. Associated production channels

The isorate curves for the $h \rightarrow \gamma\gamma$ channel in the associated production combining the $qq \rightarrow Wh$ and $q\bar{q}/gg \rightarrow t\bar{t}h$ processes are shown in Fig. 13 in the maximal-mixing scenario. The branching ratio for the $W \rightarrow \ell\nu_\ell$ decay is included. The $qq \rightarrow Wh$ process dominates the production and is large at small $\tan\beta$, enhancing the total rate in this region. The cross section of the associated production is not sensitive to the mixing and stop mass effects. The production rate can be only affected through the loop mediated $h \rightarrow \gamma\gamma$ decay process.

In the SM, the $H \rightarrow \gamma\gamma$ decay channel has been shown to be accessible in the associated $qq \rightarrow WH$ production process with an integrated luminosity of 100 fb^{-1} [26]. The total production rate required for a 5σ statistical significance in the $H \rightarrow \gamma\gamma$ decay channel is between 0.8 and 0.6 fb for $110 < m_H < 127 \text{ GeV}/c^2$. In the MSSM such a rate is expected only in the region of large m_A and small $\tan\beta$ as can be seen from Fig. 13. The $H \rightarrow b\bar{b}$ decay channel has been investigated in the associated $q\bar{q} \rightarrow t\bar{t}H$ process [27]. A 5σ statistical significance is reached in the SM with integrated luminosities exceeding 40 fb^{-1} around $m_H \sim 120 \text{ GeV}/c^2$ [27]. Due to the enhanced $h \rightarrow b\bar{b}$ couplings at large $\tan\beta$, a significant region has been shown to be covered with this decay channel in the MSSM [31].

5. Weak gauge boson fusion production channels

The SM Higgs boson is expected to be accessible in the weak gauge boson fusion production process $qq \rightarrow qqH$ for $m_H \lesssim 150 \text{ GeV}/c^2$ with the $H \rightarrow \gamma\gamma$ [32], $H \rightarrow WW^* \rightarrow \ell^+ \ell^- \nu_\ell \nu_\ell$ [33] and $H \rightarrow \tau^+ \tau^-$ [28] decay channels for integrated luminosities exceeding $\sim 60 \text{ fb}^{-1}$. For the $H \rightarrow \gamma\gamma$ decay channel the total rate required with

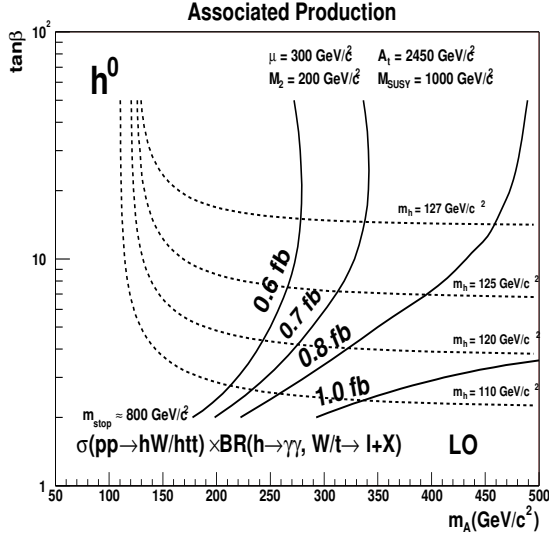


Figure 13. Isorate curves for $h \rightarrow \gamma\gamma$ in the associated production processes $q\bar{q} \rightarrow Wh$ and $q\bar{q}/g\bar{g} \rightarrow t\bar{t}h$ with $\gamma\gamma\ell$ final states. Maximal stop mixing and LO cross sections assumed.

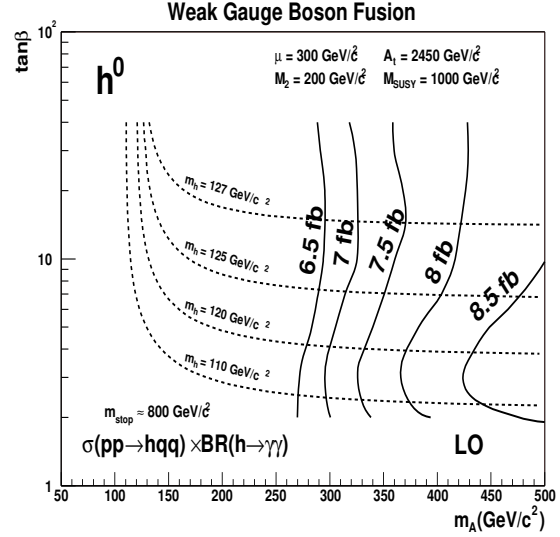


Figure 14. Isorate curves for weak gauge boson fusion $q\bar{q} \rightarrow qqh$, $h \rightarrow \gamma\gamma$ with maximal stop mixing.

60 fb^{-1} is about 8 fb for $m_H = 115 \text{ GeV}/c^2$ and 6.6 fb for $m_H = 127 \text{ GeV}/c^2$ [32]. The $H \rightarrow \tau^+\tau^-$ channel has been studied with lepton-plus-jet final states [28]. The total rate required for a 5σ statistical significance with an integrated luminosity of 30 fb^{-1} varies from 0.4 to 0.28 fb for $115 < m_H < 127 \text{ GeV}/c^2$ and from 0.28 to 0.19 fb in the interval of $127 < m_H < 145 \text{ GeV}/c^2$ for the searches of the SM-like heavy scalar H . Figures 14 and 15 show the isorate curves for the $h \rightarrow \gamma\gamma$ and $h \rightarrow \tau^+\tau^-$ decay channels in the weak gauge boson fusion process in the maximal-mixing scenario with LO cross sections. Figure 16 shows the corresponding isorate curves for the heavy scalar MSSM Higgs boson H in the $H \rightarrow \tau^+\tau^-$ decay channel. As can be seen from Fig. 15, the $h \rightarrow \tau^+\tau^-$ channel could be accessible in a large part of the parameter space already with low integrated luminosities. A sensitivity at large m_A and $\tan\beta$ is expected also in the $h \rightarrow WW^* \rightarrow \ell^+\ell^-\nu_\ell\nu_\ell$ decay channel because the studies in the SM framework indicate a 5σ discovery for $m_H \gtrsim 120 \text{ GeV}/c^2$ [33].

6. Discovery potential

Figures 17 and 18 show the discovery potential of CMS for the lightest MSSM Higgs boson as a function of m_A and $\tan\beta$ assuming maximal stop mixing, $m_{\text{top}} = 175 \text{ GeV}/c^2$ and $M_{\text{SUSY}} = 1 \text{ TeV}/c^2$, for 30 fb^{-1} and 100 fb^{-1} , respectively. The $h \rightarrow \gamma\gamma$ and $h \rightarrow ZZ^* \rightarrow \ell^+\ell^-\ell^+\ell^-$ decay channels in the inclusive production are shown with NLO cross sections. With an integrated luminosity of 100 fb^{-1} these channels cover a major part of the MSSM parameter space, for $m_A \gtrsim 200 \text{ GeV}/c^2$ and $m_A \gtrsim 250 \text{ GeV}/c^2$,

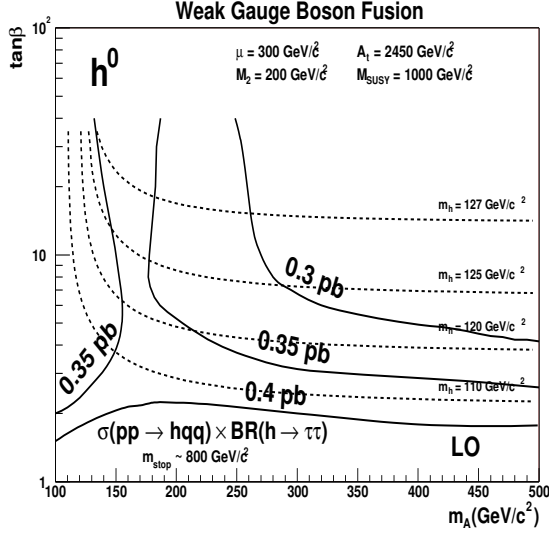


Figure 15. Isorate curves for $h \rightarrow \tau^+ \tau^-$ in the weak gauge boson fusion $qq \rightarrow qqh$. Maximal stop mixing and LO cross sections are assumed.

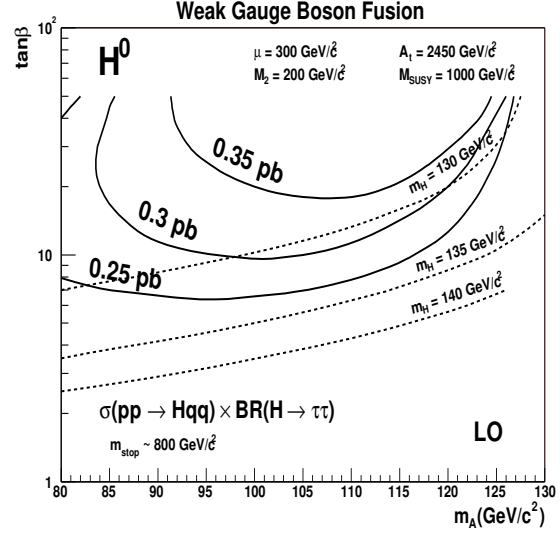


Figure 16. Isorate curves for $H \rightarrow \tau^+ \tau^-$ in the weak gauge boson fusion $qq \rightarrow qqH$ in the region of the $(m_A, \tan\beta)$ parameter space where H is SM-like. Maximal stop mixing and LO cross sections are assumed.

respectively. In the associated $qq \rightarrow Wh$ production the $h \rightarrow \gamma\gamma$ channel covers only a small region at large m_A and small ($\lesssim 5$) $\tan\beta$ values. The sensitivity for the $h \rightarrow b\bar{b}$ channel in the associated $q\bar{q}/gg \rightarrow t\bar{t}h$ production with 60 fb^{-1} from Ref. [31] is also shown in the figure. The reach in the $h \rightarrow \gamma\gamma$ and $h \rightarrow \tau^+ \tau^-$ decay channels in the weak gauge boson fusion production is shown in Fig. 17 for 60 and 30 fb^{-1} , respectively. In this production mode, the region $\tan\beta \gtrsim 5$ can be covered with the $h \rightarrow \gamma\gamma$ channel for $m_A \gtrsim 350 \text{ GeV}/c^2$ and with the $h \rightarrow \tau^+ \tau^-$ channel for $m_A \gtrsim 120 \text{ GeV}/c^2$. The $H \rightarrow \tau^+ \tau^-$ decay channel of the heavy scalar, shown also in Fig. 17, covers the region $m_A \lesssim 125 \text{ GeV}/c^2$ in the weak gauge boson fusion. The region $90 \text{ GeV}/c^2 \lesssim m_A \lesssim 130 \text{ GeV}/c^2$ at large $\tan\beta$, where the lightest Higgs boson is no more SM-like, is outside the reach of the channels discussed in this paper. To explore this region, the $h \rightarrow \mu^+ \mu^-$ and $h \rightarrow \tau^+ \tau^-$ decay channels can be used in the associated production with b quarks, $q\bar{q}/gg \rightarrow b\bar{b}h$, exploiting the enhanced couplings to down type fermions in the MSSM at large $\tan\beta$.

7. Conclusions

The production of the lightest MSSM Higgs boson h was studied, effects of SUSY parameters were discussed. The discovery potential was evaluated for CMS in the maximal-mixing scenario for the inclusive $h \rightarrow \gamma\gamma$ channel, for the $h \rightarrow \gamma\gamma$ channel in

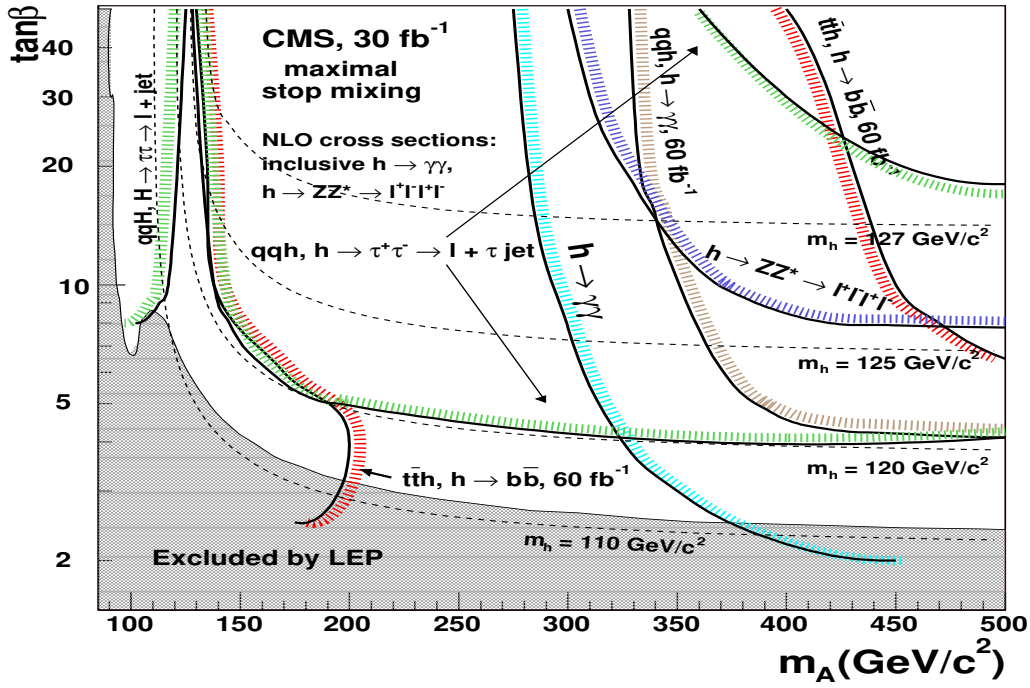


Figure 17. The 5σ -discovery potential of CMS for the lightest MSSM Higgs boson as a function of m_A and $\tan\beta$ for 30 fb^{-1} with maximal stop mixing. The reach in the $qq \rightarrow qqh, h \rightarrow \gamma\gamma$ channel is shown for 60 fb^{-1} . The discovery potential for the $t\bar{t}h, h \rightarrow b\bar{b}$ channel for 60 fb^{-1} is taken from Ref. [31]. The reach of the $H \rightarrow \tau^+\tau^-$ decay channel of the heavy scalar in the $qq \rightarrow qqH$ production process is also shown.

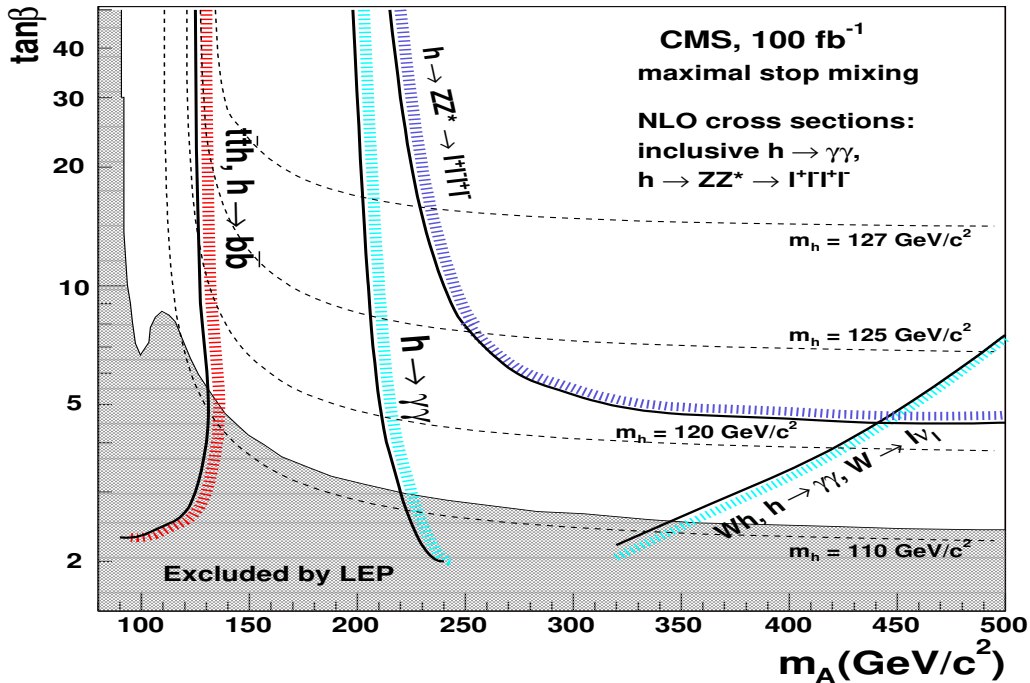


Figure 18. The 5σ -discovery potential for the lightest MSSM Higgs boson as a function of m_A and $\tan\beta$ for 100 fb^{-1} with maximal stop mixing. The discovery potential for the $t\bar{t}h, h \rightarrow b\bar{b}$ channel is taken from Ref. [31].

the associated production Wh and $t\bar{t}h$, for the $h \rightarrow \tau^+\tau^-$ channel in the weak gauge boson fusion and, for the first time, for the $h \rightarrow ZZ^* \rightarrow \ell^+\ell^-\ell'^+\ell'^-$ channel at large $\tan\beta$. Consequences of a light stop quark were shown for the expected discovery regions.

Already with an integrated luminosity of 30 fb^{-1} the parameter space $m_A \gtrsim 150 \text{ GeV}/c^2$ and $\tan\beta \gtrsim 5$, apart from a small region at large m_A and $\tan\beta$, is covered with the $h \rightarrow \tau^+\tau^-$ decay channel in the weak gauge boson fusion $qq \rightarrow qqh$. The reach with the $h \rightarrow \gamma\gamma$ decay channel with 30 fb^{-1} is for $m_A \gtrsim 300 \text{ GeV}/c^2$ in the inclusive production and for $m_A \gtrsim 350 \text{ GeV}/c^2$ in the $qq \rightarrow qqh$ production process. With 60 fb^{-1} the parameter space $150 \lesssim m_A \lesssim 400 \text{ GeV}/c^2$ ($m_A \gtrsim 150 \text{ GeV}/c^2$ for $\tan\beta \lesssim 5$) is covered with the $h \rightarrow b\bar{b}$ decay channel in the $q\bar{q}/gg \rightarrow t\bar{t}h$ production process. With the large integrated luminosity of 100 fb^{-1} the inclusive $h \rightarrow \gamma\gamma$ channel yields a 5σ -discovery for $m_A \gtrsim 200 \text{ GeV}/c^2$ and the $h \rightarrow ZZ^* \rightarrow \ell^+\ell^-\ell'^+\ell'^-$ channel for $m_A \gtrsim 250 \text{ GeV}/c^2$, $\tan\beta \gtrsim 5$.

The effects of loop corrections to the cross sections and branching ratios were studied in a scenario with large mixing and light stop quark. The consequences of the stop-top interference effects were shown for the $h \rightarrow \gamma\gamma$ decay channel in the gluon fusion and in the inclusive production. The reduction of the total production rate was found to be significant for $m_{\text{stop}} \lesssim 300 \text{ GeV}/c^2$. For $m_{\text{stop}} \lesssim 200 \text{ GeV}/c^2$ the sensitivity in the inclusive $h \rightarrow \gamma\gamma$ channel could be entirely lost. In this scenario the production rate is slightly enhanced for the associated production processes $q\bar{q}/gg \rightarrow t\bar{t}h$ and $qq \rightarrow Wh$ and in the weak gauge boson fusion $qq \rightarrow qqh$ process due to the positive interference effects on the $h \rightarrow \gamma\gamma$ decay width.

8. Acknowledgments

The authors would like to thank Michael Spira for helpful comments and for his efforts in developing the program HIGLU compatible with the other programs used in this work. P.S. and S.L. would also like to thank Katri Huitu for helpful discussions.

- [1] S. Heinemeyer and G. Weiglein, Leading Electroweak Two-Loop Corrections to Precision Observables in the MSSM, *J. High Energy Phys.* 10 (2002) 072, M. Carena and H. Haber, Higgs boson theory and phenomenology, hep-ph/0208209, *Prog.Part.Nucl.Phys.*50:63-152,2003.
- [2] LEP Higgs Working Group, Searches for the Neutral Higgs Bosons of the MSSM, hep-ex/0107030.
- [3] Combination of the CDF and D0 results on the top quark mass, hep-ex/0404010.
- [4] The LEP Higgs Working Group, http://lephiggs.web.cern.ch/LEPHIGGS/papers/August2004_MSSM/LHWG-Note-2001-01.ps.
- [5] A. Djouadi, Squark effects on Higgs boson production and decay at the LHC, hep-ph/9806315 and references therein.
- [6] DELPHI Collaboration, Searches for supersymmetric particles in e^+e^- collisions up to 208 GeV and interpretation of the results within MSSM, CERN-EP/2003-007.
- [7] LEP SUSY Work Group
http://lepsusy.web.cern.ch/lepsusy/www/squarks_summer02/squark.ps.gz.
- [8] R. Demina, J.D. Lykken, K. Matchev and A. Nomerotski, *Phys. Rev.* D62 (2000) 035011.
- [9] M. Carena, S. Heynemeyer, C.E.M. Wagner and G. Weiglein, Suggestions for improved benchmark scenarios for Higgs-boson searches at LEP2, CERN-TH/99-374, DESY 99-186, hep-ph/9912223; M. Carena, S. Heynemeyer, C.E.M. Wagner and G. Weiglein, Suggestions for Benchmark

- Scenarios for MSSM Higgs Boson Searches at Hadron Colliders, hep-ph/0202167 and references therein.
- [10] R. Kinnunen, S. Lehti, A. Nikitenko and S. Rantala, Effects of large mixing and light stop for $h \rightarrow \gamma\gamma$ in MSSM, CMS Note 2000/043.
 - [11] T. Plehn, D.L. Rainwater and D. Zeppenfeld, A method identifying $H \rightarrow \tau+\tau \rightarrow e+\mu+p(T)$ at the CERN LHC, FERMILAB-PUB-99-290-T, 1999.
 - [12] S. Abdullin et al., Summary of the CMS Potential for the Higgs Boson Discovery, CMS NOTE-2003/033.
 - [13] M. Spira, HIGLU, hep-ph/9510347.
 - [14] A.Djouadi, J. Kalinowski and M. Spira, HDECAY: a Program for Higgs Boson Decays in the Standard Model and its Supersymmetric Extension, Comput. Phys. Commun. 108 (1998) 56.
 - [15] M. Spira, <http://mspira.home.cern.ch/mspira/proglist.html>
 - [16] M.Spira *et. al.*, Nucl.Phys. B 453 (1995) 17-82.
 - [17] S. Dawson *et. al.*, hep-ph/9603423 "QCD Corrections to SUSY Higgs Production: The Role of Squark Loops".
 - [18] J. Ellis and D. Rudaz, Phys. Lett. B128 (1983) 248.
 - [19] A.Djouadi, Phys. Lett. B435 (1998) 101.
 - [20] A. Djouadi *et. al.*, The coupling of the lightest SUSY Higgs on two photons in the decoupling regime, Eur. Phys. J. C 1, 149-162 (1998).
 - [21] R. Harlander, Supersymmetric Higgs Production at the Large Hadron Collider, hep-ph/0311005.
 - [22] L3 Collaboration, Phys. Lett. B580 (2004) 37-49.
 - [23] CMS Collaboration, The Electromagnetic Calorimeter Project, Technical Design Report, CERN/LHCC 97-33, CMS TDR 4, 1997.
 - [24] CMS Collaboration, The Tracker Project, Technical Design Report, CERN/LHCC 98-6, CMS TDR 5, 1998.
 - [25] CMS Collaboration, The Muon Project, Technical Design Report, CERN/LHCC 97-32, CMS TDR 3, 1997.
 - [26] M.N. Dubinin, V.A. Ilyin and V.I. Savrin, Light Higgs Boson Signal at LHC in the Reactions $pp \rightarrow \gamma\gamma + \text{jet}$ and $pp \rightarrow \gamma\gamma + \text{lepton}$, CMS NOTE 1997/101; S. Abdullin et al., Phys. Lett., **B431** (1998) 410.
 - [27] V. Drollinger, Th. Muller and D. Denegri, Searching for Higgs Bosons in Association with Top Quark Pairs in the $H \rightarrow b\bar{b}$ Decay Mode, CMS NOTE 2001/054, hep-ph/0111312; V. Drollinger, Th. Muller and D. Denegri, Prospects for Higgs Bosons Searches in the Channel $W^\pm H \rightarrow \ell b\bar{b}$, CMS NOTE 2002/006, hep-ph/0201249.
 - [28] G. Azuelos et al., Search for the SM Higgs boson using vector boson fusion at the LHC, Workshop on Physics at TeV Colliders, Les Houches, France, 2001, hep-ph/0203056.
 - [29] I. Iashvili, R. Kinnunen, A. Nikitenko and D. Denegri, Study of the $H \rightarrow ZZ^* \rightarrow \ell^+ \ell^- \ell'^+ \ell'^-$ Channel in CMS, CMS TN/95-059.
 - [30] K. Lassila-Perini, Dissertation, ETH No. 12961 (1998).
 - [31] V. Drollinger, Private communication.
 - [32] M. Dubinin, Higgs Boson Signal in the Reaction $pp \rightarrow \gamma\gamma + \text{two Forward Jets}$, CMS NOTE 2001/022.
 - [33] N. Akchurin et al., Study of Low Mass Higgs Using $pp \rightarrow q\bar{q}H$ at CMS, CMS NOTE-2002/016.